

Cell Reports, Volume 29

Supplemental Information

**Single-Cell Profiling Defines Transcriptomic
Signatures Specific to Tumor-Reactive versus
Virus-Responsive CD4⁺ T Cells**

Assaf Magen, Jia Nie, Thomas Ciucci, Samira Tamoutounour, Yongmei Zhao, Monika Mehta, Bao Tran, Dorian B. McGavern, Sridhar Hannenhalli, and Rémy Bosselut

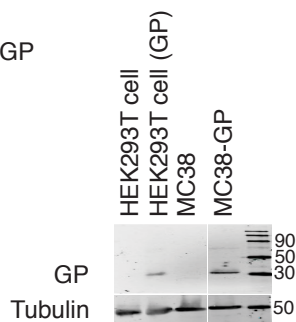
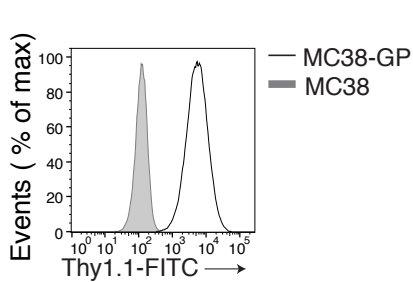
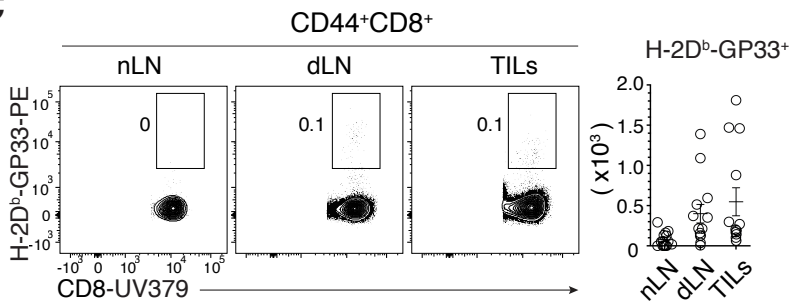
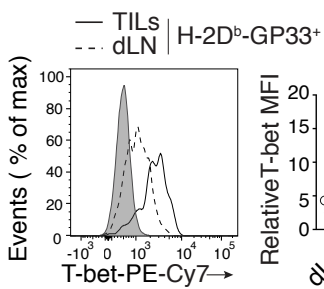
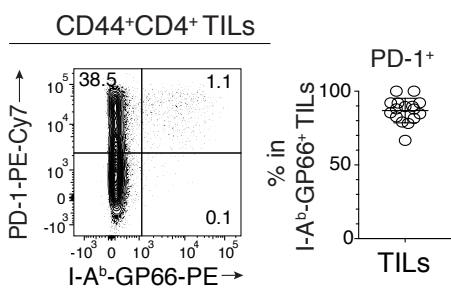
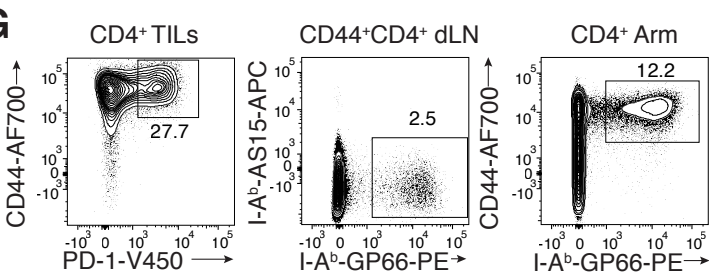
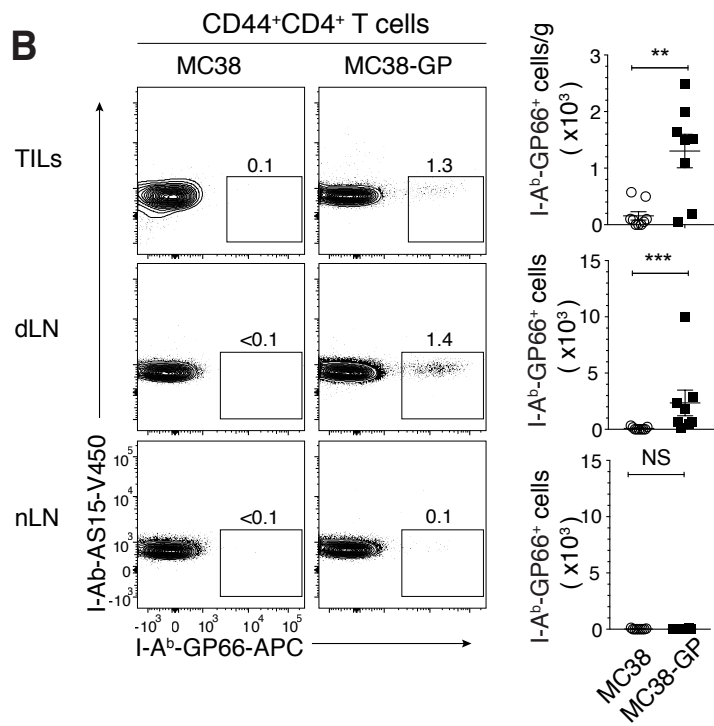
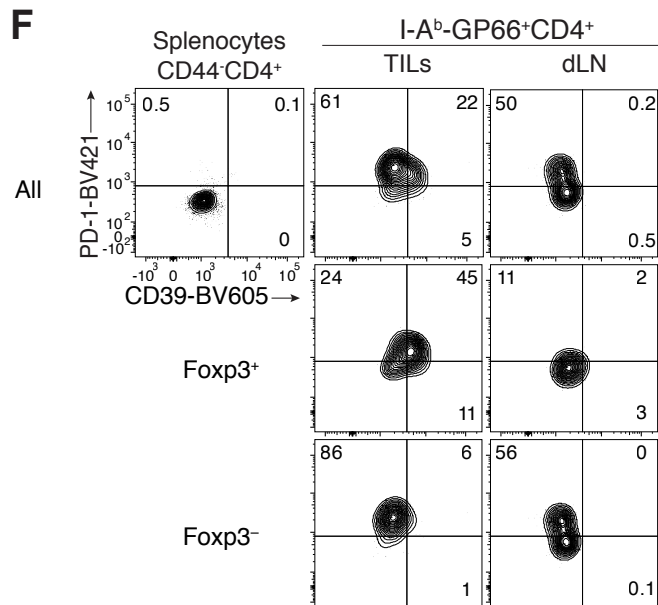
A**C****D****E****G****B****F**

Figure S1. Characterization of antigen-specific CD4⁺ T cell responses in MC38 colon adenocarcinoma tumors, Related to Figure 1.

(A) Overlaid protein expression of Thy1.1 in MC38 and MC38-GP cells (left). Immunoblot analysis of GP protein expression in HEK293T cells, HEK293T cells transfected with pMRX-GP-IRES-Thy1.1 plasmid, MC38 cells or MC38-GP cells (right).

(B) C57BL/6 mice were subcutaneously injected MC38 or MC38-GP cells and analyzed at day 14 post-injection. Left panel shows flow cytometry contour plots of GP66 vs. control (AS15 peptide from *T. gondii*) class II tetramer staining in TILs, dLN and nLN from MC38 and MC38-GP tumor-bearing mice. Right panel shows the number of GP66⁺ TILs per gram of tumor and total number of GP66⁺ dLN and nLN cells, separately for MC38 and MC38-GP tumor-bearing mice (Unpaired Mann-Whitney U test, ** p < 0.01, *** p < 0.001, NS: not significant). Data is from 8 mice of each condition analyzed in two experiments.

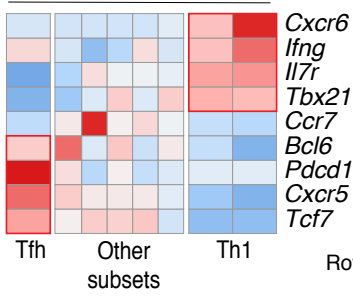
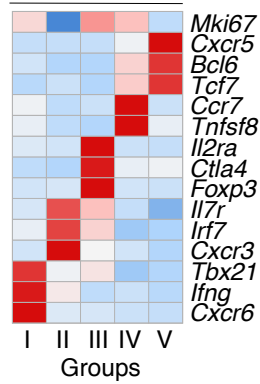
(C) Flow cytometry analysis of CD8 expression vs. GP33 class I tetramer staining in nLN, dLN and TILs from MC38-GP tumor-bearing mice (left). Total number of GP33⁺ dLN and nLN cells, and number of GP33⁺ TILs per gram of tumor (right). Data is from 13 mice analyzed in three experiments.

(D) Overlaid protein expression of Tbet in GP33⁺ CD8⁺ dLN and TILs; grey shaded histogram shows Tbet expression in naive CD8⁺ splenocytes from tumor-free control mice; histogram shows concatenated data from 6 individual mice analyzed in one experiment. Graph on the right shows Tbet MFI in GP33⁺ dLN and TILs; data is from 9 tumor bearing mice analyzed in two experiment and is expressed relative to naive CD8⁺ splenocytes from tumor-free control mice. Each symbol represents an individual mouse.

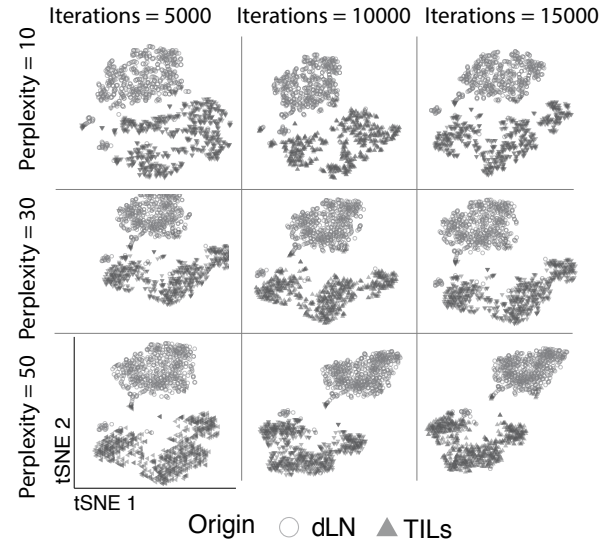
(E) Flow cytometry contour plots of GP66 tetramer vs. PD-1 staining in TILs (left) and percentage of PD-1⁺ cells out of GP66⁺ TILs (right). Data is from 16 mice analyzed in three experiments.

(F) Right two columns show flow cytometry expression of PD-1 vs. CD39 in GP66⁺CD4⁺ TILs or dLN, gated on all such cells (top row) or Foxp3⁺ or Foxp3⁻ subsets (bottom rows). Top left plot shows staining of naive splenocytes from tumor-free mice. Data is representative from 11 mice analyzed in three experiments.

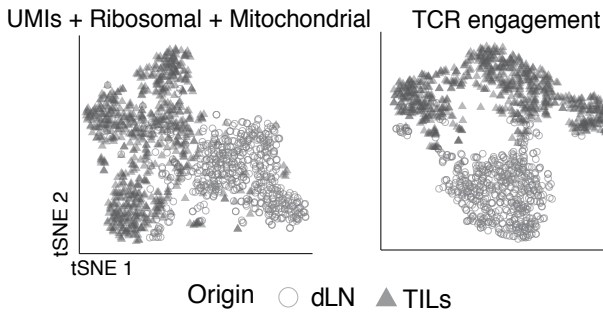
(G) GP66-specific CD44^{hi} CD4⁺ splenocytes were isolated from WT animals 7 days post-infection with LCMV Armstrong. Protein expression contour of populations used for scRNAseq captures from MC38-GP tumor-bearing mice (TILs PD-1 vs. CD44, dLN GP66 vs. AS15 control) and LCMV Armstrong infected mice (GP66 vs. CD44). Data is representative from >50 mice analyzed in >10 experiments.

AGP66⁺CD44⁺CD4⁺ Arm**B**CD44⁺CD4⁺ TILs and dLN**C**

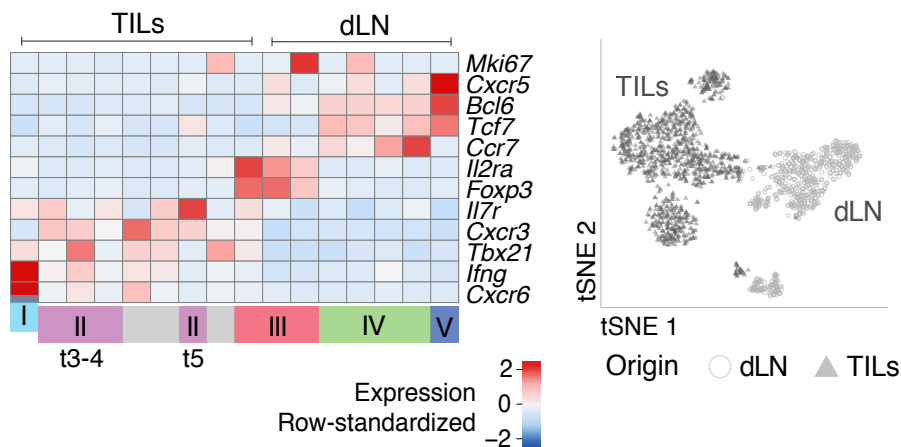
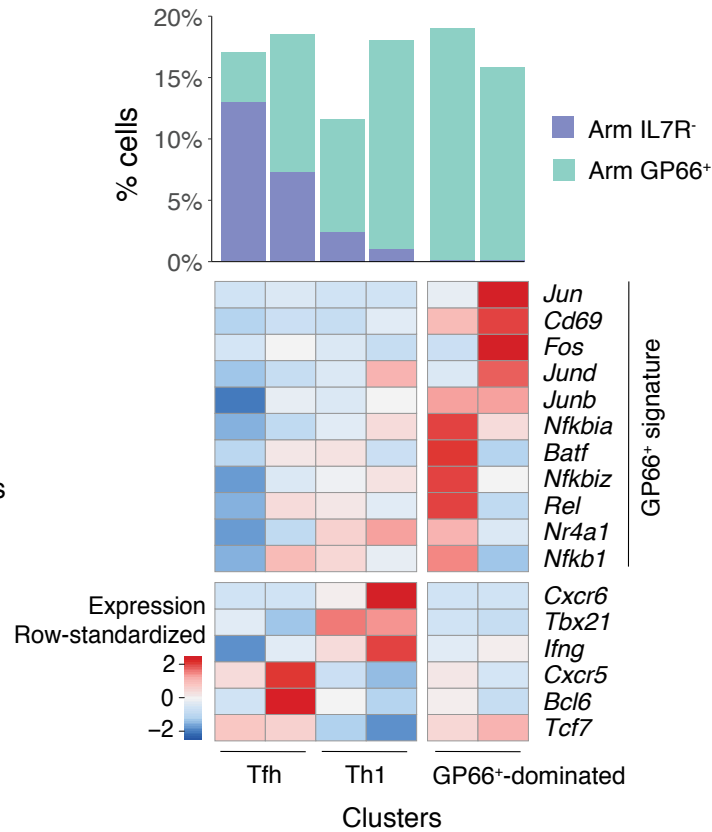
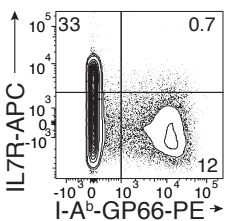
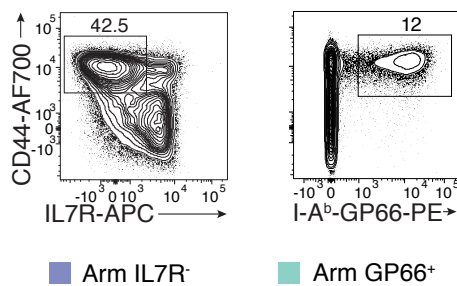
TILs and dLN

**D**

TILs and dLN

**E**

TILs and dLN replicate experiment II

**H**CD44⁺CD4⁺ T cells**F**CD4⁺ Arm**G**CD4⁺ Arm

■ Arm IL7R⁻ ■ Arm GP66⁺

Figure S2. Characterization of immune responses to Arm and MC38-GP by scRNAseq, Related to figures 1 and 2.

(A) GP66-specific CD4⁺ splenocytes from WT animals 7 days post-infection with LCMV Armstrong analyzed by scRNAseq. Heatmap shows row-standardized expression of selected genes across Arm clusters.

(B-E) TILs and dLN cells from WT mice at day 14 post MC38-GP injection analyzed by scRNAseq. **(B)** Heatmap shows row-standardized expression of selected genes across main TIL and dLN groups (as defined in text). **(C)** tSNE display of TILs and dLN cells generated using different parameter combination of perplexity and number of iterations, grey-shaded by tissue origin. **(D)** tSNE displays of TILs and dLN cells, grey-shaded by tissue origin, post confounder correction for number of unique molecular identifiers (UMIs) and expression of ribosomal and mitochondrial coding genes (left) or TCR engagement on dLN cells as a result of GP66-tetramer-based purification (right). **(E)** scRNAseq analysis of TILs and dLN cells from replicate experiment II. Heatmap shows row-standardized expression of selected genes across TIL and dLN clusters (left). tSNE display of TILs and dLN cells, grey-shaded by tissue origin (right).

(F-H) Analysis of CD4⁺ splenocytes from C57BL/6 animals 7 days post-infection with LCMV Armstrong (Arm). **(F)** Flow cytometry contour plot of GP66 tetramer staining vs. IL7R in CD4⁺ Arm cells. **(G)** Flow cytometry contour plots of IL7R vs. CD44 (for Arm IL7R⁻ sample, **left**) and GP66 vs. CD44 (for Arm GP66⁺ sample, **right**). **(H)** Arm IL7R⁻ and Arm GP66⁺ cells analyzed by scRNAseq. Heatmap shows row-standardized expression of selected genes across pooled Arm IL7R⁻ and Arm GP66⁺ clusters (**bottom**). Bar plot indicates the number of Arm IL7R⁻ and Arm GP66⁺ cells in each cluster relative to the total number of cells (**top**).

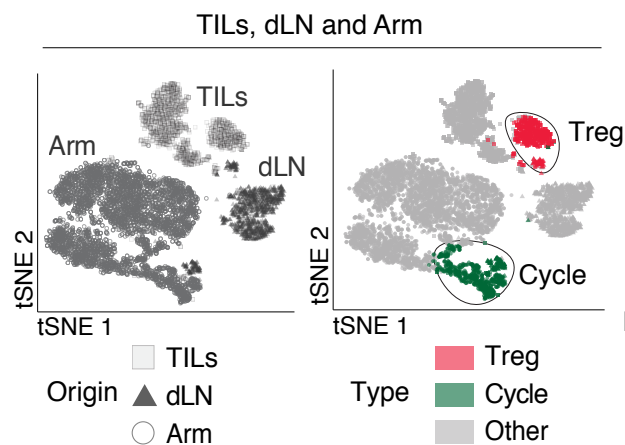
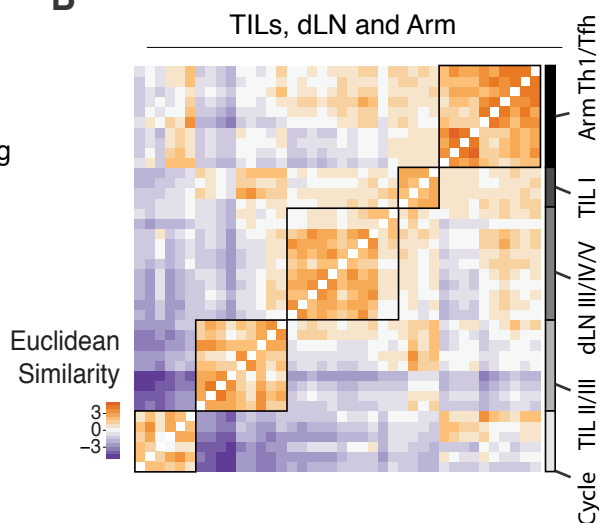
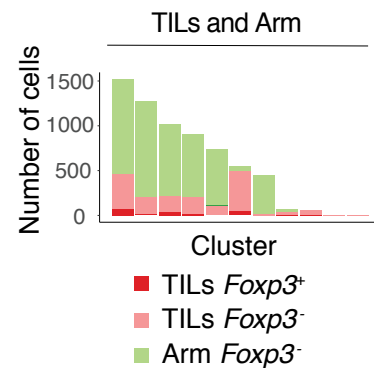
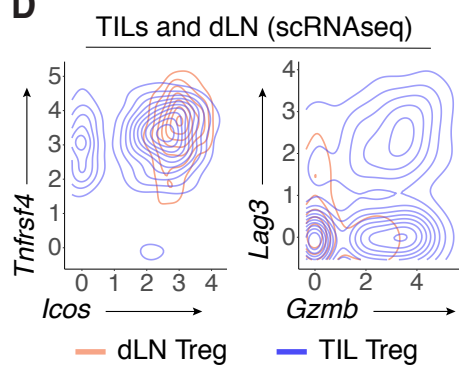
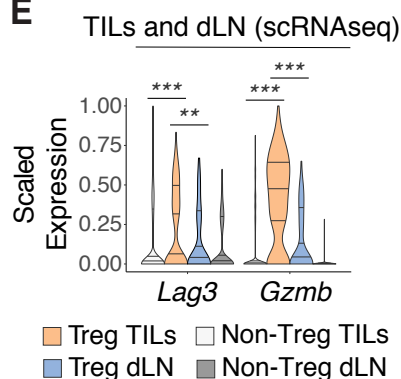
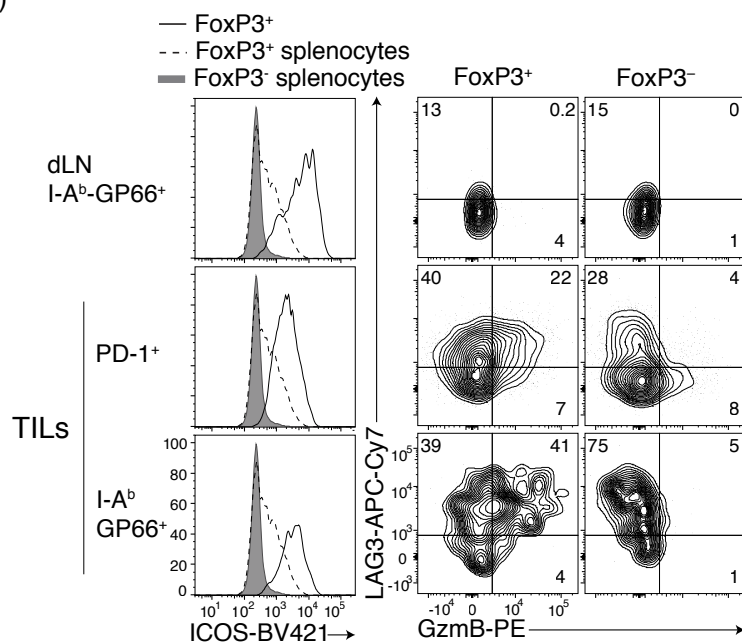
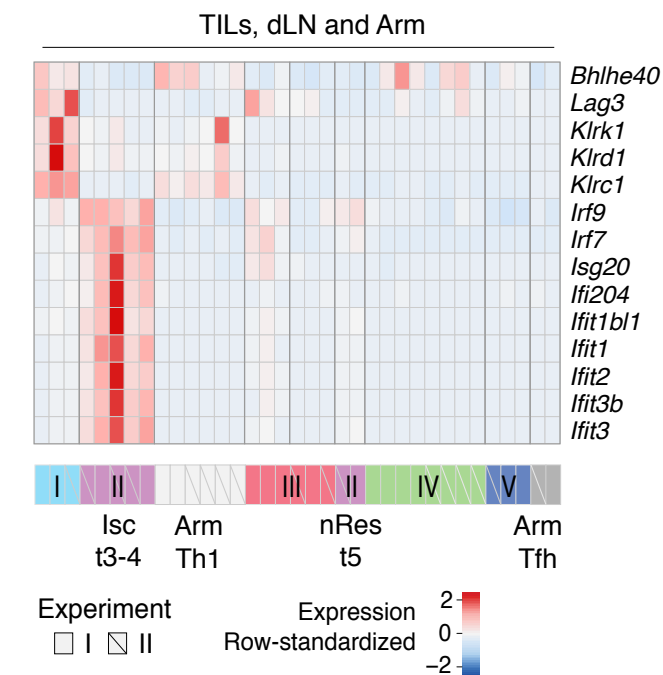
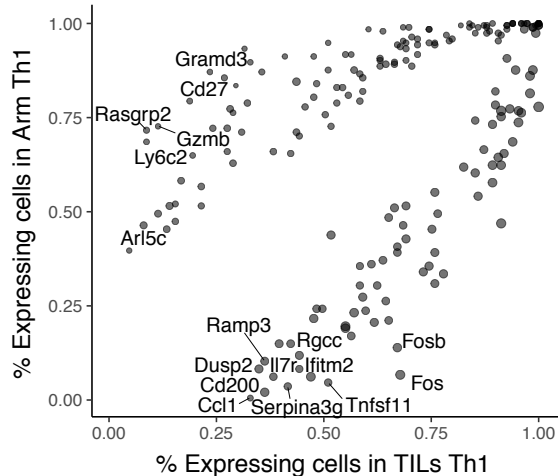
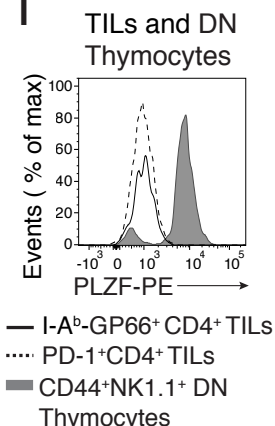
A**B****C****D****E****F****G****H****I**

Figure S3. Assessment of tissue-context-specific effects on clustering analyses and TILs-dLN heterogeneity, Related to Figure 3.

(A-C, G,H) TILs, dLN and Arm cells from replicate experiments I and II analyzed by scRNAseq. **(A)** tSNE plots show TILs, dLN, and Arm cells, grey-shaded by origin (left) or color-coded by Treg or cell-cycle (Cycle) clustering assignment (grey for all other clusters) (right). **(B)** Heatmap shows Euclidean similarity between cluster-specific average expression vectors (as defined in text) (left) annotated with cluster origin and cluster group or type (right). **(C)** Bar plot shows relative cluster composition of Foxp3⁺ or Foxp3⁻ TILs and Foxp3⁻ Arm (no Foxp3⁺ cells found in GP66⁺ Arm) after applying a data integration approach (Butler et al., 2018).

(D-E) Comparison of dLN Tregs and TIL Tregs (respectively clusters t6-7 and n1 as shown in Fig. 1A). **(D)** Contour plots of dLN Treg (orange) or TIL Treg (blue) cell distribution according to scRNAseq-detected normalized expression of *Icos* vs. *Tnfrsf4* (left) and *Gzmb* vs. *Lag3* (right). **(E)** Violin plot of *Lag3* and *Gzmb* scRNAseq expression in Treg vs. non-Treg TIL and dLN populations (Unpaired T test, ** p < 0.01, *** p < 0.001); bands indicate quartiles (25th, 50th and 75th quantile).

(F) Overlaid flow cytometry expression of ICOS in Foxp3⁺ TILs and dLN cells and Foxp3⁺ or Foxp3⁻ CD4⁺ splenocytes from tumor-free control mice (left). Data is representative from 11 mice analyzed in three experiments. Flow cytometry contour plots of Granzyme B vs. LAG3 in Foxp3⁺ TILs or Foxp3⁺ dLN cells (middle), and Foxp3⁻ TILs or Foxp3⁻ dLN (right). Graphs were generated from 5 concatenated files, each of them representing a single mouse and processed in parallel in one experiment. Data is representative of 2 such experiments.

(G) Heatmap shows row-standardized expression of TIL Isc and Th1 characteristic genes across TIL, dLN and Arm clusters.

(H) Gene detection statistics (% expressing cells) of differentially expressed genes by scRNAseq in TILs Th1 and Arm Th1.

(I) Overlaid protein expression of PLZF in GP66⁺ and PD-1⁺ TILs and CD44^{hi} NK1.1⁺ DN (double negative CD4⁻CD8⁻) thymocytes from tumor-free control mice. Data is representative from 10 mice analyzed in two experiments.

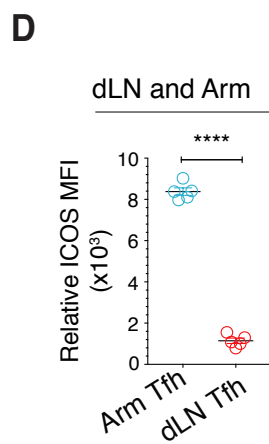
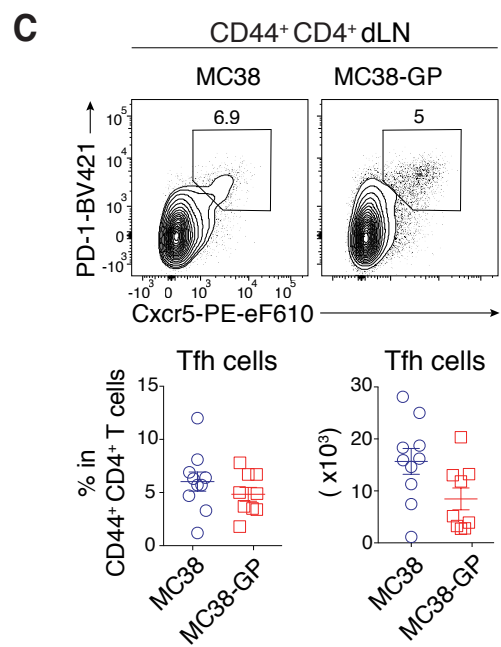
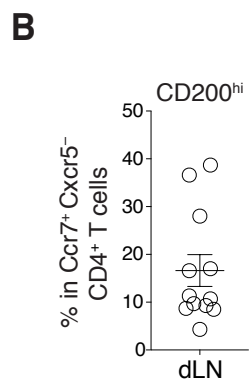
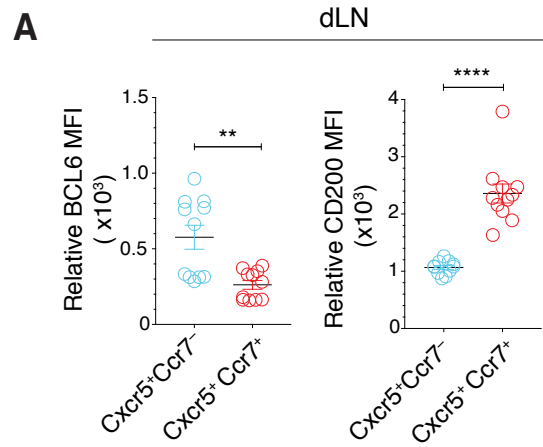


Figure S4. dLN cell diversity, Related to Figure 4.

(A) Mean fluorescence intensity (MFI) of BCL6 and CD200 in CXCR5⁺ or CCR7⁺GP66⁺ dLN cells relative to naive CD4⁺ splenocytes from tumor-free control mice. (Unpaired t-test, ** p < 0.005, **** p < 0.0001).

(B) Percentage of CD200^{hi} cells out of CCR7⁺CXCR5⁺ dLN cells.

(C) Top panel shows flow cytometry contour plots of CXCR5 vs. PD-1 in CD44^{hi} CD4⁺ dLN cells from MC38 and MC38-GP tumor-bearing mice. Bottom panel shows percentage of Tfh cells out of total CD44^{hi} CD4⁺ T cells in dLN (left) and total number of Tfh cells (right). (A-C) Data is representative of 17 mice analyzed in three experiments.

(D) Mean fluorescence intensity (MFI) levels of ICOS in Arm Tfh and dLN Tfh relative to naive CD4⁺ splenocytes from tumor-free control mice (Unpaired t-test, p < 10⁻⁵). (A-C) Data is representative of 10 mice analyzed in two experiments.

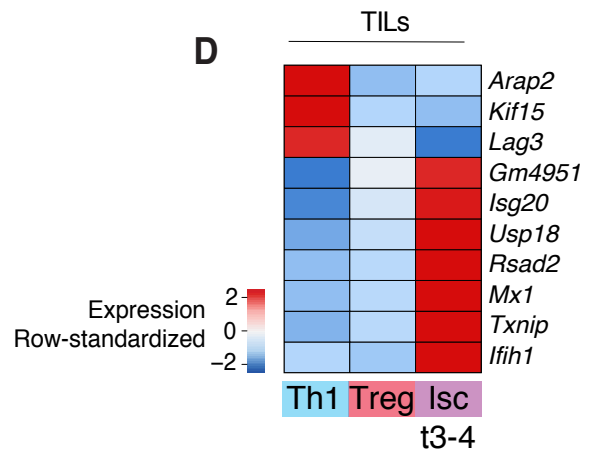
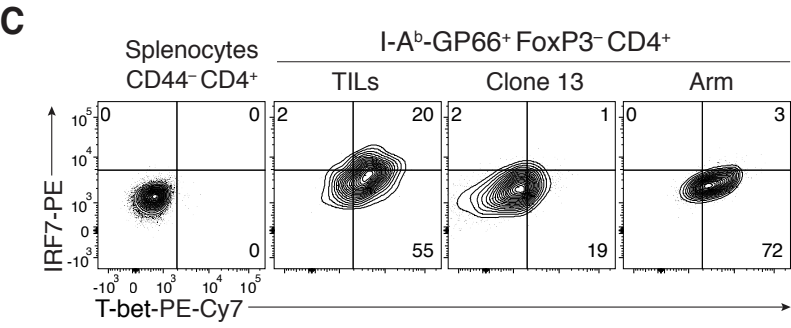
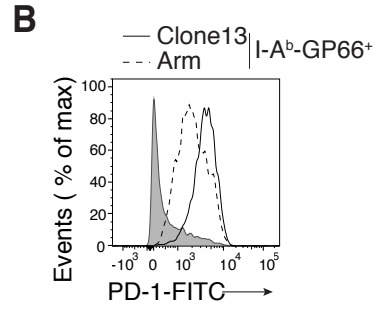
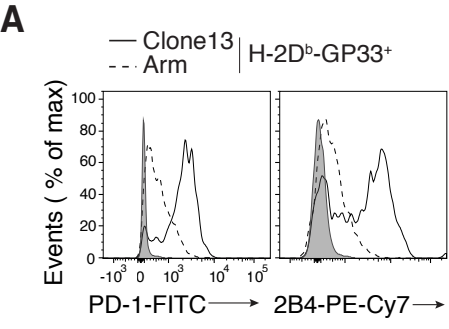


Figure S5. Characterization of the exhaustion status in clone 13 cells and TILs, Related to Figure 5.

(A) Overlaid protein expression of PD-1 or 2B4 in GP33⁺ CD8⁺ splenocytes from Arm- or Clone 13-infected mice.

(B) Overlaid protein expression of PD-1 in GP66⁺ CD4⁺ splenocytes from Arm- or Clone 13-infected mice. Grey shaded trace (A, B) is control from tumor-free mice.

(C) Flow cytometry contour plots of Tbet vs. IRF7 in Foxp3 GP66⁺ TILs, Clone 13, or Arm cells, and in naive CD4⁺ splenocytes from tumor-free control mice. (A-C) Data is representative of 10 mice analyzed in two experiments.

(D) Heatmap shows row-standardized expression of selected exhaustion genes across TIL Th1, Treg and Isc clusters (respectively clusters t1-2, t6-7 and t3-4 as shown in Fig. 1A).

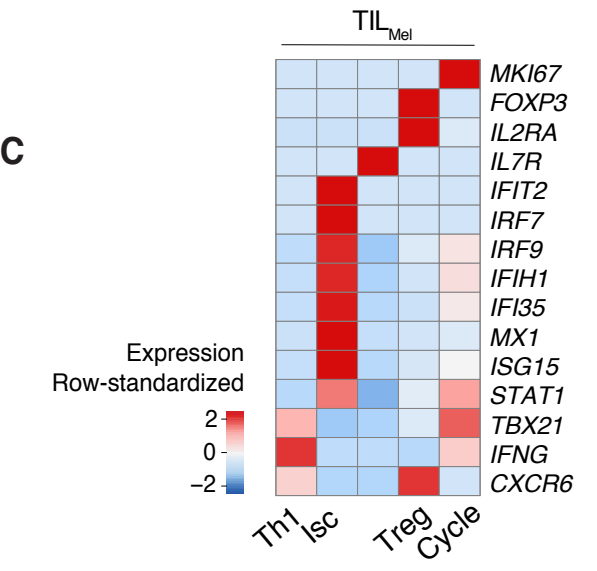
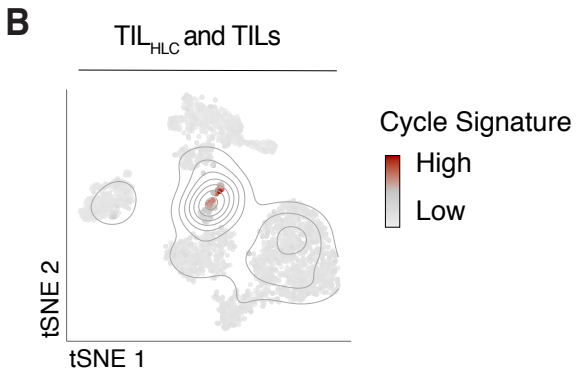
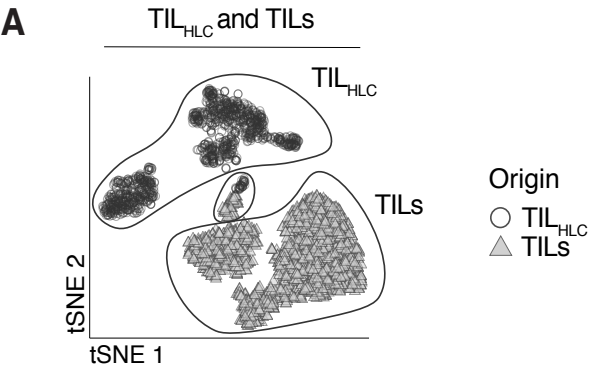


Figure S6. Correspondence to human data and dysfunction gene signatures, Related to Figure 6.

(A-B) Analysis of TIL_{HLC} and TIL_S (as defined in text). **(A)** tSNE plots show cells grey-shaded by origin. **(B)** tSNE plots show cells color-coded by cell cycle signature activation level.

(C) Analysis of TIL_{Mel} (as defined in text). Heatmap shows row-standardized expression of selected TIL characteristic genes across TIL_{Mel} clusters.